




RESEARCH ARTICLE | JULY 24 2023

## Triply differential cross sections for electron and positron impact on methane **FREE**

Prithvi Singh ; Vijay Bagul ; Christophe Champion 



*J. Chem. Phys.* 159, 044302 (2023)

<https://doi.org/10.1063/5.0149844>



View  
Online



Export  
Citation

CrossMark



**The Journal of Chemical Physics**  
**Special Topic: Adhesion and Friction**

**Submit Today!**



# Triply differential cross sections for electron and positron impact on methane

Cite as: J. Chem. Phys. 159, 044302 (2023); doi: 10.1063/5.0149844

Submitted: 9 March 2023 • Accepted: 3 July 2023 •

Published Online: 24 July 2023



View Online



Export Citation



CrossMark

Prithvi Singh,<sup>1,a)</sup>  Vijay Bagul,<sup>1</sup>  and Christophe Champion<sup>2</sup> 

## AFFILIATIONS

<sup>1</sup>Department of Physics, School of Engineering, Sir Padampat Singhanian University, Bhatewar, Udaipur, Rajasthan 313601, India

<sup>2</sup>Centre d'Études Lasers et Applications (CELIA), Université de Bordeaux, 33400 Talence, France

<sup>a)</sup>Author to whom correspondence should be addressed: [prithvipurohit@gmail.com](mailto:prithvipurohit@gmail.com)

## ABSTRACT

We here report theoretical triply differential cross sections (TDCS) for 250 eV electron and positron impact ionization of the methane molecule calculated within the second-order distorted-wave Born approximation (DWBA2) for various momentum transfer conditions. The experimental data taken from Işık *et al.* [J. Phys. B: At., Mol. Opt. Phys. 49, 065203 (2016)] will be compared with the current theoretical predictions as well as molecular three body distorted wave (M3DW) approximation and generalized Sturmian function (GSF) theoretical models in a non-coplanar geometry. In the low analyzer scattering plane, the results obtained within the DWBA2 theory show better agreement with the experimental results compared to the GSF results. The M3DW results also exhibit agreement with the experimental results, in particular in the perpendicular plane geometry. Furthermore, significant differences between electron and positron TDCS were observed.

Published under an exclusive license by AIP Publishing. <https://doi.org/10.1063/5.0149844>

## I. INTRODUCTION

The electron-impact ionization dynamics of atoms and molecules has been of great interest in a wide range of research areas, including the simulation of laboratory plasmas and planetary atmospheres, the analysis of astrophysical data, and the understanding of results in radiation chemistry and biology.

In this context, the triply differential cross section (TDCS) has emerged as a useful tool for understanding the whole dynamics of the ( $e, 2e$ ) collision mechanism of single ionization via electron impact. Indeed, the TDCS provides the most accurate information regarding the ionization process since all the specifics of the impact have been taken into account.<sup>2,3</sup> In recent years, great progress has been made in understanding the ionization mechanism that occurs when charged particles (electron/positron) interact with simple and complex atomic and molecular targets. However, the many-body problem remains unsolved. Various theoretical models and approximations have then been proposed, and experiments play a crucial role in validating the accuracy of the theoretical approximations.<sup>4-6</sup>

In recent years, the theory has made significant progress by defining the dynamics of electron-impact ionization of atomic hydrogen, helium, and other atoms with one or two electrons in their

outer shells. The interactions are defined by several close coupling strategies, such as convergent close coupling (CCC), R-matrix methods, time-dependent close coupling (TDCC), and external complex scaling (ECS).<sup>7-10</sup> More complex targets (such as rare gases) are far more difficult to deal with, particularly at low incident energy levels, but considerable progress has been made. The R-matrix technique also provides fairly good agreement with argon ionization experimental data,<sup>11</sup> which uses comparable kinematic settings as neon experiments.

The pseudo-state B-spline R matrix approach and the three-body distortion wave (3DW) approximation exhibit outstanding agreement with the whole three-dimensional neon ionization experimental data at very low incident electron energy.<sup>12</sup> The challenge of single ionization of molecular targets is complicated by the target's multicenter character. In theory, the target multi-center character should be taken into account in both the initial and final channels. To simplify the many body difficulties into a manageable three-body problem, the standard technique consists of representing the target as a one-active electron target, with the remaining electrons being considered passive actors. As a result, the multi-center elements of the collision must be taken into consideration when calculating the active electron wave function in both the initial and final channels.

In order to calculate the bound state wave function for the active state wave, multi-center effects must be taken into consideration in the incident channel.

The ideal approach consists of using a single-center expansion to mimic the active electron bound state wave functions. In this context, many numerical codes exist that may provide a detailed description of the molecular ground state in terms of linear combinations of atomic orbitals (LCAOs), a simple technique that has been proven to provide reasonably accurate results. In addition, another computing technique, namely, the density functional theory (DFT) approach,<sup>26</sup> provides very accurate results but requires more computational resources to be effectively used in practical applications. In the final channel, the multi-center nature problem is commonly approximated as an effective charge or a screened effective charge positioned near the center of mass. Thus, the continuous electron flows in an effective field formed by the remnant ionic core, screened by the other passive electrons of the target, in the Distorted-Wave-Born Approximation (DWBA).

The multi-center effect is taken into account by using the molecular three-body distortion wave (M3DW) approach, which uses spherically symmetric effective electron charge distributions and a nuclear potential that is dependent on the position of the nucleus relative to the center of mass.<sup>13–18</sup> The generalized Sturmian function (GSF) approach, which was originally designed for atoms, was adapted for the handling of tiny polyatomic molecules and expanded to the investigation of single ionization by photon and electron impact.<sup>19–22</sup>

In this work, we investigate methane (CH<sub>4</sub>) electron-impact ionization at moderate incidence energies. CH<sub>4</sub> is the most common greenhouse gas created on Earth as a result of human and animal activity, and it is linked to climate change and global warming.

Within the second-order distorted wave Born approximation (DWBA2) formalism, the effect of projectile charge on the triply differential cross sections in coplanar asymmetric kinematics for electron- vs positron-induced ionization of the CH<sub>4</sub> molecule for a relatively low incident energy of 81 eV is investigated. The enhanced version of the distorted wave Born approximation (DWBA) is the second-order distorted wave Born approximation (DWBA2). The phenomena of electron exchange, post-collisional interaction (PCI), and the correlation-polarization effect have all been considered.

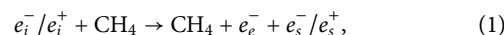
The DWBA2 computations also provided are compared to the experimental results<sup>26</sup> as well as the theoretical predictions from the molecular three-body distorted wave approximation (M3DW) and GSF.<sup>26</sup>

In Sec. II, we briefly report on the theoretical model and discuss its validity in Sec. III in comparison with experiments.

Atomic units are used throughout unless otherwise indicated.

## II. THEORY

The single ionization of the methane molecule (CH<sub>4</sub>) by electron and positron impacts is defined as



where  $e_i^-/e_i^+$  refers to the incident electron/positron,  $e_e^-$  to the ejected electron, and  $e_s^-/e_s^+$  to the scattered electron/positron.

### A. The methane molecular wave functions

The molecular orbitals of the methane target are expressed in terms of Slater-like functions that are all centered on a common origin,<sup>23</sup>

$$\Psi_i(r) = \sum_{j=1}^{N_i} a_j \varphi_{n_j l_j m_j}^{\xi_j}(r), \quad (2)$$

where  $N_i$  refers to the number of Slater orbitals and  $a_{ij}$  is the weight of each atomic component  $\varphi_{n_j l_j m_j}^{\xi_j}(r)$ .

The molecular orbitals are then described as

$$\varphi_{n_j l_j m_j}^{\xi_j}(r) = R_{n_j l_j}^{\xi_j}(r) S_{l_j m_j}^{\xi_j}(\hat{r}), \quad (3)$$

where  $R_{n_j l_j}^{\xi_j}(r)$  corresponds to the radial part of the wave function with

$$R_{n_j l_j}^{\xi_j}(r) = \frac{(2\xi_j)^{2n_j+1/2}}{\sqrt{n_j!}} r^{n_j-1} e^{-\xi_j r} \quad (4)$$

and  $S_{l_j m_j}^{\xi_j}(\hat{r})$  to the angular part expressed in terms of solid harmonics<sup>24</sup> that are related to complex harmonics by

$$\begin{cases} \text{if } m_j \neq 0 \Rightarrow S_{l_j m_j}^{\xi_j}(\hat{r}) = \left(\frac{m_j}{2|m_j|}\right)^{\frac{1}{2}} \left\{ Y_{l_j - |m_j|}(\hat{r}) + (-1)^{m_j} \left(\frac{m_j}{|m_j|}\right) Y_{l_j |m_j|}(\hat{r}) \right\} \\ \text{if } m_j = 0 \Rightarrow S_{l_j m_j}^{\xi_j}(\hat{r}) = Y_{l_j |m_j|}(\hat{r}) \end{cases} \quad (5)$$

where  $\hat{r}$  indicates the solid angle direction.

### B. The DWBA2 description of the electron-impact ionization process

The triply differential cross section of the methane molecule ionization is calculated by using the second-order distorted wave Born approximation (DWBA2) method as follows:

$$\frac{d^3\sigma}{d\Omega_s d\Omega_e dE_e} = (2\pi)^4 \frac{k_s k_e}{k_i} \sum_{av} |f_{B_1} + f_{B_2}|^2, \quad (6)$$

where  $d\Omega_e = \sin\theta_e d\theta_e d\varphi_e$  and  $d\Omega_s = \sin\theta_s d\theta_s d\varphi_s$  denote the solid angles of the ejected and scattered electrons, respectively, while  $k_i$ ,  $k_s$ , and  $k_e$  refer to the momentum of the incident, the scattered, and the ejected electrons, respectively.

The first- and second-order distorted wave Born approximations are, respectively, given by

$$f_{B_1} = \left\langle \chi_1^{(-)}(k_s, r_1) \chi_2^{(-)}(k_e, r_0) \right. \\ \left. \times \left| - \left( \frac{z}{r_1} - \frac{1}{|r_1 - r_0|} \right) \right| \Psi_i(r_0) \chi_0^{(+)}(k_i, r_1) \right\rangle \quad (7)$$

and

$$f_{B_2} = \langle \chi^{(-)}(k_s, r_1) \chi^{(-)}(k_e, r_0) | V G_0^+ V | \Psi_i(r_0) \chi_0^{(+)}(k_i, r_1) \rangle, \quad (8)$$

where  $Z$  denotes the ionized target charge (here  $Z = 1$ ) and  $G_0^+$  is the Green's function defined as

$$G_0^+ = \frac{1}{E_0 - H + i\epsilon}, \quad (9)$$

where  $H$  is the Hamiltonian of the target described by

$$H = -\frac{\nabla^2}{2} \pm \left( \frac{Z}{r_1} - \frac{1}{|r_1 - r_0|} \right) \text{ and } \epsilon \rightarrow 0^+. \quad (10)$$

The distorted wave function is invoked by the incident wave function  $\chi_0^{(+)}(k_i, r_1)$  while the two outgoing wave functions  $\chi_1^{(-)}(k_s, r_1)$  and  $\chi_2^{(-)}(k_e, r_0)$  invoke the distorted wave function.

### C. The DWBA2 description of the positron-impact ionization process

The cross-section is created by a positron beam striking a methane molecule. With a positive (+) sign, the amplitude of the first and second order expressions changes as follows:

$$f_{B_1} = \left\langle \chi_1^{(-)}(k_s, r_1) \chi_2^{(-)}(k_e, r_0) \right. \\ \left. \times \left| + \left( \frac{z}{r_1} - \frac{1}{|r_1 - r_0|} \right) \right| \Psi_i(r_0) \chi_0^{(+)}(k_i, r_1) \right\rangle, \quad (11)$$

$$f_{B_2} = \langle \chi^{(-)}(k_s, r_1) \chi^{(-)}(k_e, r_0) | V G_0^+ V | \Psi_i(r_0) \chi_0^{(+)}(k_i, r_1) \rangle. \quad (12)$$

The distorted wave for the incident positron is used to calculate the neutral distorting potential; the distorted wave for the scattered positron is used to calculate the ion potential; and the distorted wave for the ejected electron is used to calculate the static exchange potential of molecular ions.

### D. The post collision interaction (PCI)

The post-collision interaction (PCI) and distorted wave Born approximation (DWBA) are calculated by using the Ward–Macek factor.<sup>25</sup> The following equation describes the relationship between the projectile electron and the ejected electron:

$$|C_{proj-eject}|^2 = G |F_1(i\gamma, 1, -2ik_{ab}r_{ab}^{ave})|^2, \quad (13)$$

where  $G$  is described as

$$G = \left| e^{-\frac{\pi\gamma}{2}} \Gamma(1 - i\gamma) \right|^2 = \frac{\pi/k_{ab}}{(e^{\pi/k_{ab}} - 1)}, \quad (14)$$

where  $\Gamma$  refers to the Gamma function,  $k_{ab}$  is the relative electron–electron wave number, which depends on the relative velocity  $v_{ab}$ , and  $\gamma$  is the Sommerfeld parameter defined by  $\gamma = z_p \frac{z_e}{v_{ab}}$  where  $z_e$  and  $z_p$  are the ejected electron and projectile electron charges, respectively.

The average separation is given by

$$r_{ab}^{ave} = \frac{\pi^2}{16\epsilon} \left( 1 + \frac{0.627}{\pi} \sqrt{\epsilon \ln \epsilon} \right)^2, \quad (15)$$

where  $\epsilon$  refers to the total energy of the two emerging electrons.

Finally, the TDCS expression incorporating post-collision interaction (using the Ward–Macek factor) is given by

$$\frac{d^3\sigma}{d\Omega_1 d\Omega_2 dE_2} = |C_{proj-eject}|^2 (2\pi)^4 \frac{k_1 k_2}{k_0} \sum_{av} |f_{B_1} + f_{B_2}|^2. \quad (16)$$

## III. RESULTS AND DISCUSSION

In Fig. 1, triply differential cross-sections for electron–positron impact ionization of CH<sub>4</sub> (outer valence molecular orbitals 1t<sub>2</sub>) are illustrated, with an incident energy of 250 eV and an ejected electron energy of 50 eV.

The DWBA2 triply differential cross sections for electron impact (red solid line) and positron impact (blue solid line) were compared to measurements (solid circles) as well as to the molecular three-body distorted wave (M3DW) (dotted line) and the Generalized Sturmian Functions (GSF) approach predictions<sup>26</sup> (dashed–dotted line).

We first observe that all the theoretical results (DWBA2, M3DW, and GSF) exhibit a similar behavior that is in very good agreement with the experimental data for the three fixed analyzer angle values (10°, 20°, and 25°) [panels (a)–(c), respectively]. More precisely, we observe that all the theoretical results show the binary region, as experimentally observed in the structure of the TDCS.

For the two smaller analyzer angles (10° and 20°), the experimental<sup>1</sup> and current DWBA2 calculations, as well as the M3DW calculations, both have a peak localized at an angle that is greater than the momentum transfer direction, which could be due to the electron–electron repulsion in the final state, namely, the interaction after the collision (PCI).

From a general point of view, we observe that the DWBA2 results are quite consistent with the experiment, except for the analyzer angle of 25° [Fig. 1(c)], where the DWBA2 results only predict the amplitude of the binary peak (solid line) that is almost identical to that observed in the measurements with, nevertheless, a small shift of its localization in comparison with the experimental results. The current DWBA2 calculations, as well as the M3DW and GSF results, show a double binary peak structure for the analyzer angle of 25° [Fig. 1(c)], similarly to the experimental results. For the two lower analyzer angles (10° and 20°), we observe a double peak in the momentum transfer direction with a fairly deep minimum for the greatest scattering angle of 25°.<sup>27–29</sup>

Finally, the most recent positron impact TDCS (blue solid curve) has shown quite similar TDCS behavior to that reported for electron impact (red solid curve). In reality, within the experimental data, the actions of electrons and positrons are indistinguishable.

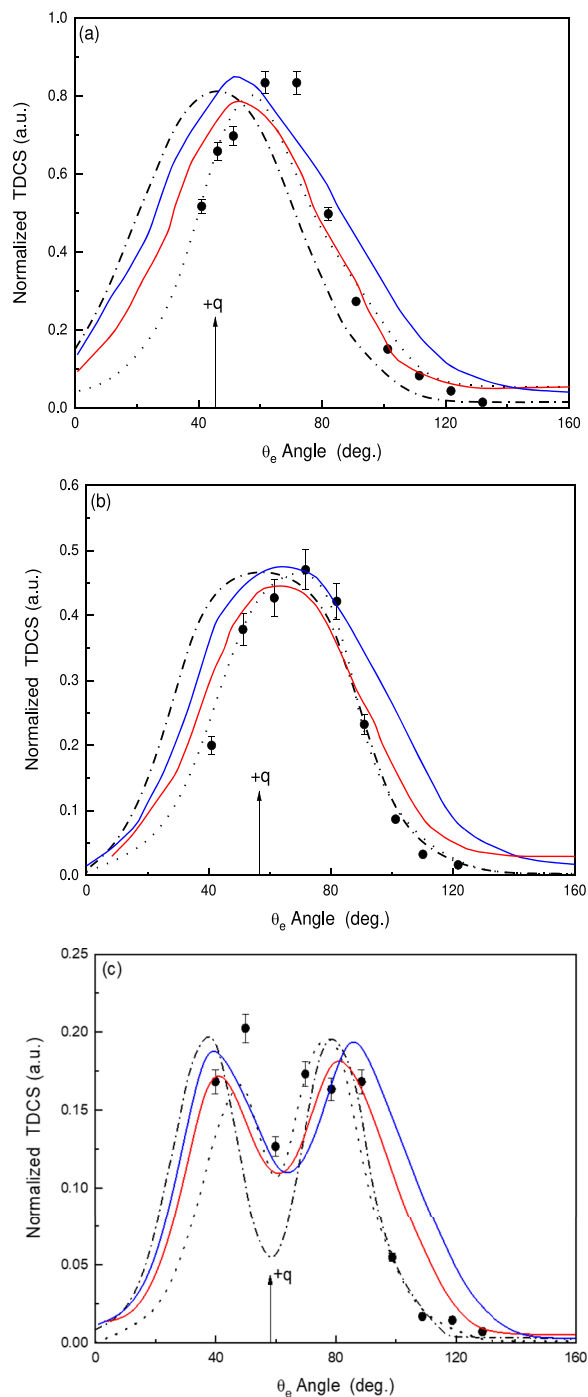


**FIG. 1.** TDCS for electron and positron ionization of  $\text{CH}_4$  molecules at 250 eV incident energy and 50 eV ejected electron energy (red solid line and blue solid line, respectively). The panels (a)–(c) show the TDCS at various analyzer angles, namely,  $10^\circ$ ,  $20^\circ$ , and  $25^\circ$ , respectively. The theoretical (DWBA2) TDCS values are compared with electron measurements (solid circles)<sup>26</sup> and two other theoretical models, namely, M3DW (dotted line) and GSF (dashed–dotted line).

In the case of atoms, similar results have also been reported in the literature.<sup>30,31</sup>

Figure 2 compares the experimental results of the Afyon group<sup>26</sup> with the theory for 30 eV ejected electrons and two fixed analyzer angles ( $10^\circ$  and  $20^\circ$ ). The DWBA2 results as well as the M3DW and GSF predictions are in relatively good agreement. When the analyzer angle is equal to  $10^\circ$  [Fig. 2(a)], the experimental binary peak is displaced to greater angles relative to the direction of momentum transfer, in good agreement with the DWBA2 and M3DW results.

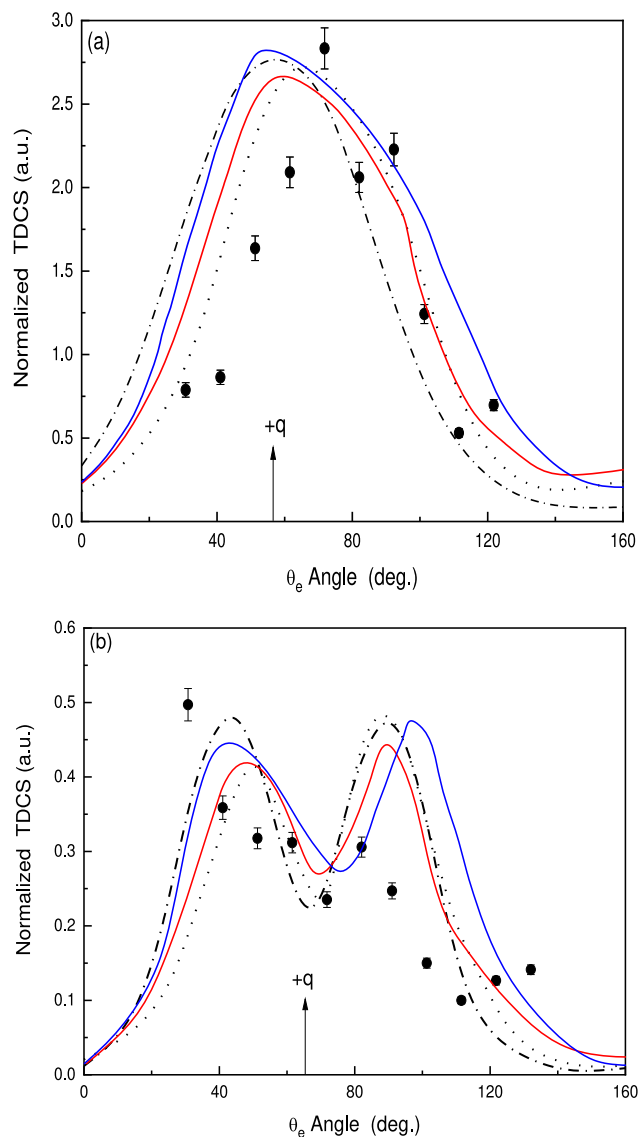


**FIG. 2.** Same as in Fig. 1 at 250 eV incident energy and 30 eV ejected electron energy for two analyzer angles [panel (a)  $10^\circ$ , panel (b)  $20^\circ$ ].

In Fig. 2(b), the single binary peak becomes a double binary peak as the scattering angle increases. This is in contrast to the theoretical result, as GSF predicts that the amplitudes of the double peaks will be equal (as a direct result of the first Born model), whereas DWBA2 and M3DW calculations suggest that the peaks will be larger at higher angles. The current positron impact TDCS (blue solid curve) is quite comparable to the electron impact TDCS (solid red curve). This is due to the post-collision interaction (PCI) between two charged particles that are similar (electron–electron) and oppositely charged (electron–positron).

In general, the DWBA2 results are more consistent with the experiments for electron impact ionization in the scattering plane. Continuum electrons are treated as waves deformed by the target Coulomb field in both calculations (DWBA2 and M3DW). The M3DW is a first-order calculation that includes all orders of perturbation theory as well as post-collision interaction (PCI), whereas the DWBA2 is a second-order calculation that approximates PCI using the Ward–Macek approximation.

When the energies of the two ejected electrons are comparable, it is likely that the post-collision interaction (PCI) appears as the dominant factor. However, in this context, the ejected electron energy ranges from 30 to 50 eV. In this context, it is clear that the PCI impact is not the main interaction. Additionally, the experimental results of this kinematics are more consistent with the DWBA2 results, showing that the second-order contribution is more substantial than the PCI contribution.

Figures 3 and 4 compare the experimental results of the Manchester group<sup>26</sup> with the current theoretical predictions for ejection

electron energies of 50 and 30 eV, respectively, with fixed analyzer angles  $\theta_a = 20^\circ, 22.5^\circ, 25^\circ, 27.5^\circ,$  and  $30^\circ$ .

First, let us note that the three theoretical sets clearly provide comparable TDCS in shape, with relative amplitudes as well as peak positions well reproduced by the DWBA2 theory, in good agreement with the experiment at all angles  $\theta_a$ .

In panel (a) ( $\theta_a = 20^\circ$ ), we get a single peak, while in panel (b) ( $\theta_a = 22.5^\circ$ ), the single peak has split into two peaks. In panel (c) ( $\theta_a = 25^\circ$ ), the single split into two peaks with a relatively deep minimum, while in panel (d) ( $\theta_a = 27.5^\circ$ ), the larger angle second peak begins to decrease compared to the second and third analyzer angles and has almost disappeared for  $\theta_a = 30^\circ$  [panel (e)]. The DWBA2 results for electron and positron impact ionization are in reasonably good agreement with the experiments as well as the M3DW results.

In Fig. 4(a) ( $\theta_a = 20^\circ$ ), we get a double-peak structure, while in Fig. 4(b) ( $\theta_a = 22.5^\circ$ ), the second peak structure decreases with the experimental results. In Fig. 4(c) ( $\theta_a = 25^\circ$ ), the higher-angle peak in the double-peak structure is already negligible, according to the experiment, while in Fig. 4(d) ( $\theta_a = 27.5^\circ$ ), the second peak is essentially eliminated, and both theories (DWBA2 and M3DW) predict that it will completely disappear  $\theta_a = 30^\circ$  [panel (e)].

Regarding the positron results (blue solid line), the double-peak structure of the TDCSs is similar to that reported for electron, with, nevertheless, a slightly different magnitude. In fact, in all cases reported in Figs. 3 and 4, the positron binary peak appears to be slightly higher than that observed with the electron binary peak.

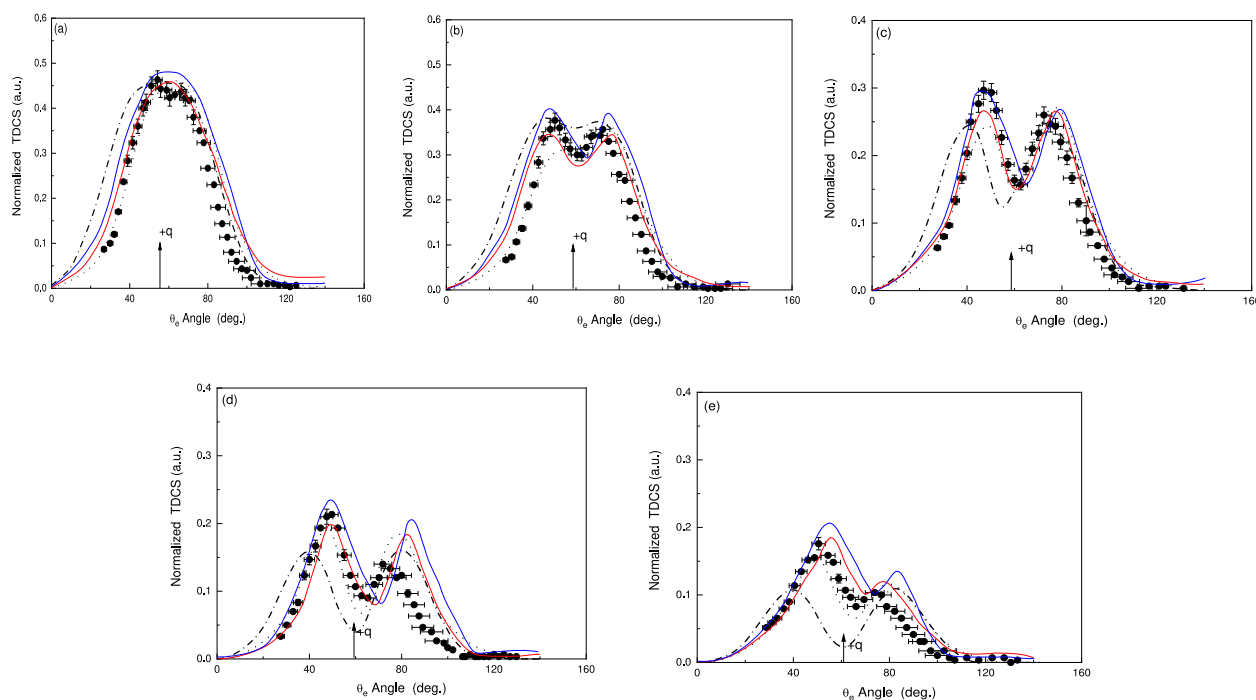


**FIG. 3.** TDCS for electron and positron ionization of  $\text{CH}_4$  molecules at 250 eV incident energy and 50 eV ejected electron energy (red solid line and blue solid line, respectively). The panels (a)–(e) show the TDCS for various analyzer angles, namely,  $20^\circ, 22.5^\circ, 25^\circ, 27.5^\circ,$  and  $30^\circ$ , respectively. The theoretical (DWBA2) TDCS values are compared with electron measurements (solid circles<sup>26</sup>) and two other theoretical models, namely, M3DW (dotted line) and GSF (dashed–dotted line).

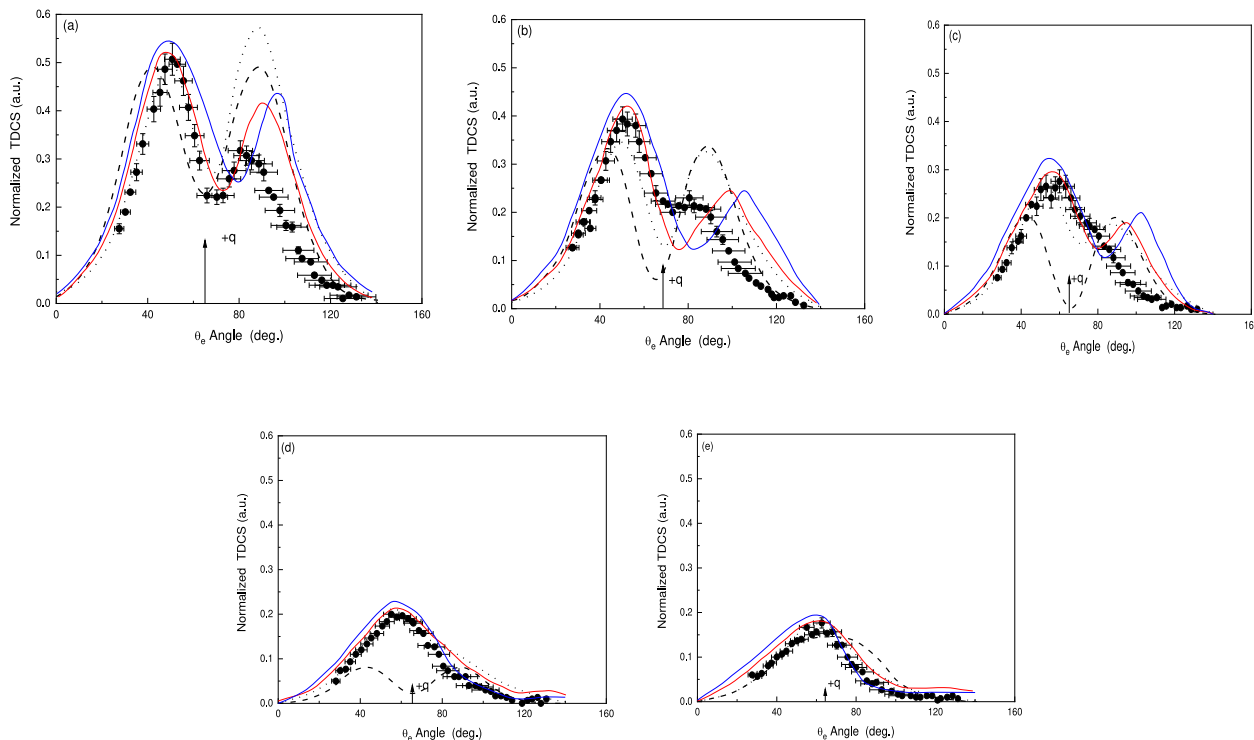


**FIG. 4.** Same as in Fig. 3 at 250 eV incident energy and 30 eV ejected electron energy for five analyzer angles [Panel (a) 20°, Panel (b) 22.5°, Panel (c) 25°, Panel (d) 27.5°, and Panel (e) 30°].

When there are two peaks, both experiments predict that the intensity of the large-angle peak is less than the intensity of the small-angle peak. The double peak intensities are the same for the GSF calculation due to symmetry, so the pattern cannot be reproduced. In contrast, two peaks with different peak intensities will be produced in the DWBA2 and M3DW calculations.

#### IV. CONCLUSIONS

TDCS for electron and positron impact ionization of the  $1t_2$  and  $2a_1$  states of the  $\text{CH}_4$  molecule has been reported by using the second-order Distorted Wave Born Approximation (DWBA2).

The DWBA2 theoretical results were compared with available experimental results for electron-impact ionization at various analyzer angle positions as well as with the previously reported GSF and molecular three-body distorted wave (M3DW) predictions.

From a general point of view, the cross-sections reported in the current work have shown very good agreement with the experiment. More precisely, the DWBA2 calculations exhibit a good agreement in shape with the experimental data for 50 eV ejected electron energy, an agreement that was less satisfactory but still fair in the case of 30 eV ejected electron energy.

Compared to the GSF calculations, the DWBA2 findings are in better overall agreement with regard to the position and the relative magnitude of the experimental peaks.

The M3DW is a theory of the first order that involves the interaction of post-collision (PCI) with all orders of perturbation theory.

The DWBA2 is a theory of the second-order, which includes PCI approximately. If both final state electrons have the same momentum, which is not the case for current kinematics, PCI should be more relevant. Consequently, the results of the scattering plane suggest that second-order is more significant for these kinematics than the long-range PCI effects.

There is still no experimental TDCS data available for the positron impact ionization of  $\text{CH}_4$  molecules. Nevertheless, for the positron projectile, we compared our results with the electron cross-sections. Our observations show that both the electron and positron TDCS are very close in shape. The electron and positron results in the scattering plane are consistent with the experimental error.

#### ACKNOWLEDGMENTS

P.S. acknowledges Sir Padampat Singhania University, Udaipur.

#### AUTHOR DECLARATIONS

##### Conflict of Interest

The authors have no conflicts to disclose.

#### Author Contributions

**Prithvi Singh:** Writing – original draft (lead). **Vijay Bagul:** Writing – original draft (supporting). **Christophe Champion:** Writing – review & editing (equal).

## DATA AVAILABILITY

The data that support the findings of this study are available within the article.

## REFERENCES

- <sup>1</sup>N. Işık, M. Doğan, and S. Bahçeli, *J. Phys. B: At., Mol. Opt. Phys.* **49**, 065203 (2016).
- <sup>2</sup>K. Bartschat and M. J. Kushner, *Proc. Natl. Acad. Sci. U. S. A.* **113**, 7026 (2016).
- <sup>3</sup>E. Alizadeh, T. M. Orlando, and L. Sanche, *Annu. Rev. Phys. Chem.* **66**, 379 (2015).
- <sup>4</sup>M. Vos, S. A. Canney, I. E. McCarthy, S. Utteridge, M. T. Michalewicz, and E. Weigold, *Phys. Rev. B* **56**, 1309 (1997).
- <sup>5</sup>M. Takahashi, N. Watanabe, Y. Khajuria, Y. Udagawa, and J. H. D. Eland, *Phys. Rev. Lett.* **94**, 213202 (2005).
- <sup>6</sup>S. Samarin, O. M. Artamonov, A. D. Sergeant, J. Krischner, A. Morozov, and J. F. Williams, *Phys. Rev. B* **70**, 073403 (2004).
- <sup>7</sup>I. Bray and A. T. Stelbovics, *Phys. Rev. A* **46**, 6995 (1992).
- <sup>8</sup>T. N. Rescigno, M. Baertschy, W. A. Isaacs, and C. W. McCurdy, *Science* **286**, 2474 (1999).
- <sup>9</sup>J. Colgan, M. S. Pindzola, and F. Robicheaux, *J. Phys. B: At., Mol. Opt. Phys.* **37**, L377 (2004).
- <sup>10</sup>O. Zatsarinny and K. Bartschat, *Phys. Rev. A* **85**, 062710 (2012).
- <sup>11</sup>X. Ren, S. Amami, O. Zatsarinny, T. Pflüger, M. Weyland, A. Dorn, D. H. Madison, and K. Bartschat, *Phys. Rev. A* **93**, 062704 (2016).
- <sup>12</sup>X. Ren, S. Amami, O. Zatsarinny, T. Pflüger, M. Weyland, W. Y. Baek, H. Rabus, K. Bartschat, D. H. Madison, and A. Dorn, *Phys. Rev. A* **91**, 032707 (2015).
- <sup>13</sup>J. M. Soler, E. Artacho, J. D. Gale, A. García, J. Junquera, P. Ordejón, and D. Sánchez-Portal, *J. Phys.: Condens. Matter* **14**, 2745 (2002).
- <sup>14</sup>R. M. Dreizler and E. K. U. Gross, *Density Functional Theory* (Springer, 1990).
- <sup>15</sup>R. G. Parr and W. Yang, *Density-Functional Theory of Atoms and Molecules* (Oxford University Press, 1994).
- <sup>16</sup>J. Gao, D. H. Madison, and J. L. Peacher, *Phys. Rev. A* **72**(2), 020701(R) (2005).
- <sup>17</sup>J. Gao, D. H. Madison, and J. L. Peacher, *J. Chem. Phys.* **123**(20), 204314 (2005).
- <sup>18</sup>S. Zhang, X. Y. Li, J. G. Wang, Y. Z. Qu, and X. Chen, *Phys. Rev. A* **89**, 052711 (2014).
- <sup>19</sup>G. Gasaneo, L. U. Ancarani, D. M. Mitnik, J. M. Randazzo, A. L. Frapiccini, and F. D. Colavecchia, *Adv. Quantum Chem.* **67**, 153 (2013).
- <sup>20</sup>C. M. Granados-Castro, “Application of generalized Sturmian basis functions to molecular systems,” Ph.D. thesis, Université de Lorraine, Metz, 2016.
- <sup>21</sup>C. M. Granados-Castro, L. U. Ancarani, G. Gasaneo, and D. M. Mitnik, *Adv. Quantum Chem.* **73**, 3 (2016).
- <sup>22</sup>C. M. Granados-Castro and L. U. Ancarani, *Eur. Phys. J. D* **71**, 65 (2017).
- <sup>23</sup>R. Moccia, *J. Chem. Phys.* **40**, 2164 (1964).
- <sup>24</sup>H. Trygve, P. Jorgensen, and J. Olsen, *Molecular Electronic Structure Theory* (John Wiley & Sons, New York, 2000).
- <sup>25</sup>S. J. Ward and J. H. Macek, *Phys. Rev. A* **49**, 1049 (1994).
- <sup>26</sup>E. Ali, C. Granados, A. Sakaamini, M. Harvey, L. U. Ancarani, A. J. Murray, M. Dogan, C. Ning, J. Colgan, and D. Madison, *J. Chem. Phys.* **150**, 194302 (2019).
- <sup>27</sup>M. A. Stevenson, L. R. Hargreaves, B. Lohmann, I. Bray, D. V. Fursa, K. Bartschat, and A. Kheifets, *Phys. Rev. A* **79**, 012709 (2009).
- <sup>28</sup>M. A. Haynes and B. Lohmann, *Phys. Rev. A* **64**, 044701 (2001).
- <sup>29</sup>C. T. Whelan, in *Fragmentation Processes: Topics in Atomic and Molecular Physics*, edited by C. T. Whelan (Cambridge University Press, 2013), pp. 223–260.
- <sup>30</sup>G. Purohit and D. Kato, *Phys. Rev. A* **96**, 042710 (2017).
- <sup>31</sup>R. I. Campeanu, J. H. R. Walters, and C. T. Whelan, *Eur. Phys. J. D* **69**, 235 (2015).